catalysts

MDPI

Article

A Theoretical Study on Pd-catalyzed, Friedel-Crafts Intermolecular Acylation: Does Generated In Situ Aroyl Triflate Act as A Reactive Electrophile to Functionalize C–H Bond of Arenes?

Rong Chang [1], Ye Tian [1], Niu Li [1], Jin Bai [1], Huimin Yan [1], Wenjing Yang [1], Zhen Guo [1,*] and Yanrong Li [2,*]

[1] College of Material Science & Engineering, Key Laboratory of Interface Science and Engineering in Advanced Materials, Ministry of Education, Taiyuan University of Technology, Shanxi 030024, China; changrong0414@foxmail.com (R.C.); Tianye1988@163.com (Y.T.); fengyuwuqing99@163.com (N.L.); share.baijin@foxmail.com (J.B.); yhm969218@sohu.com (H.Y.); wenjing130966@163.com (W.Y.)

[2] Department of Earth Science and Engineering, Taiyuan University of Technology, Shanxi 030024, China

* Correspondence: guozhen@tyut.edu.cn (Z.G.); li.dennis@hotmail.com (Y.L.); Tel.: +86-351-6010916 (Z.G.)

Received: 2 December 2018; Accepted: 16 January 2019; Published: 2 February 2019

Abstract: The mechanism of Pd-catalyzed, Friedel-Crafts intermolecular acylation of arenes to ketones was comprehensively investigated by using DFT calculations. The calculated results revealed that this transformation was composed of several key steps: C–I bond oxidative addition, CO insertion, reductive elimination and C–H bond functionalization. Of these steps, the last was found to be the rate–determining step, and it occurred much more easily with strongly electrophilic aroyl triflate compared to other resultant counterparts. In addition, our calculation provides a rationale for experimental findings that simple Pd salts exhibit superior catalytic abilities compared to phosphine-ligated Pd catalysts.

Keywords: intermolecular acylation; palladium; monoxide and C–H bond functionalization

1. Introduction

Aromatic ketones have attracted widespread attention as promising industrial materials and pharmaceutical ingredients, and have been widely employed in the various fields, for example, natural products and material science [1–3]. Several highly efficient methods for constructing valuable ketones have been established in recent years, such as the classic Friedel-Crafts acylation and metal-catalyzed acylation reactions [4–9]. In general, the classic Friedel-Crafts acylation reactions involve some high-energy electrophiles nascent from reactive reagents (e.g., $SOCl_2$ and PCl_3) [10]. Thus, they were subject to harsh reaction conditions, low selectivity and non-atomic economy. Compared to the classic Friedel-Crafts reactions, metal-catalyzed acylation reactions are rapidly evolving and widely used for inactivated C–H bond functionalization, and have many advantages of high functional group tolerance, atomic economy and mild reaction conditions. In this regard, transition metal-catalyzed carbonylative cross-coupling reactions to ketones, in which monoxide was utilized as a carbonyl source, have been extensively investigated and reported (Scheme 1) [11,12]. However, they were also limited by requisites of pre-synthesized organometallic agents, substrates with directing groups and activated substrate, especially in the intermolecular carbonylative events. As such, the development of new, efficient methodologies to promote related acylation reactions is highly desirable.

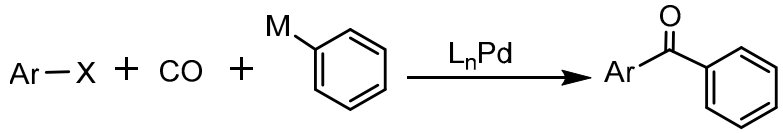

Scheme 1. Transition metal-catalyzed carbonylative cross-coupling reactions to ketones.

Recently, Arndtsen B.A. and co-workers reported a novel approach to form ketones through palladium-catalyzed intermolecular carbonylation of arene C–H bonds in the presence of CO as the carbonyl sources [13]. These reactions exhibited high yields, very low palladium catalyst loadings and high functional group tolerance, in which directing groups, pre-synthesized organometallic reagents and ligands were not employed, and a strongly reactive electrophilic agent was generated in situ (e.g., aroyl triflate). Such catalytic reductive carboxylation reactions are very important, because they have provided a previously unexplored route for the preparation of ketones using readily available aryl iodides, CO and arenes. This route also offers a straightforward and green alternative to Friedel-Crafts reactions via carbon monoxide to generate in situ, high-energy electrophiles.

The experimental results reported by Arndtsen B.A. et al. demonstrated that the reactivity was strongly dependent on whether ligands were employed or not in the carbonylative reactions (Scheme 2). For example, Pd catalysts that contained phosphine ligands, such as P^tBu_3, resulted in the carbonylative functionalization of benzene into ketone in low yields, whereas the simple Pd salts without added ligands, such as $PdCl_2$, resulted in higher yields (up to 99%). These findings are very interesting and raise a number of underlying reaction mechanistic questions for the titled reaction, which can be summarized as follows: (1) how was the aroyl triflate generated in situ? (2) Is the in situ-generated aroyl triflate adequately reactive to functionalize the inactivated C–H bond of arenes? (3) Why are simple Pd salts superior to the Pd catalysts containing phosphine ligands in term of reactivity? To address these issues, we conducted DFT calculations to gain further insight into the reaction mechanism with the aim of facilitating the development of synthetic catalysts for CO incorporation, and to provide in-depth guidance for synthetic chemists on the related intermolecular carbonylative coupling reactions.

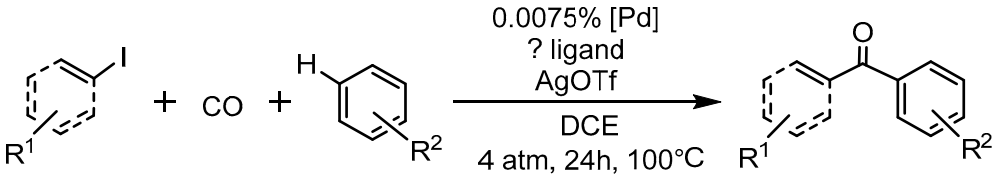

Scheme 2. Pd-catalyzed, Friedel-Crafts intermolecular acylation with arene to ketones.

2. Computational Details

All calculations were performed with the G09 package [14]. The geometric optimization of all complexes was carried out at the B3LYP/6–31G(d) level [15–19] of theory in which effective core potential(ECP) type basis set SDD [20,21] was applied on Pd, Ag and I atoms. With the same level of theory and basis set, vibrational analysis was performed to confirm all the stationary points as local minima or transition states and provide the thermal corrections to the single point energies in solution. Intrinsic reaction coordination (IRC) calculations were used to verify the connections among the transition states and its reactant and product [22]. The solvent effect from dichloroethane was considered based on single-point calculations of the gas phase stationary points using a SMD [23] continuum solvation model and by the M06 functional [24–26] with SDD basis set for Pd, Ag and I and 6–311++G(d,p) [27] basis set for the rest of the atoms. This computational method (B3LYP for optimization)//(M06 for single point energy in solution) has proved more reliable in energy for metal-catalyzed reactions [28–32], especially for systems containing transition metal elements and weak intermolecular interactions [24–26]. Unless otherwise stated, all discussed energies in what follows refer to solvation free energy (ΔG_{sol}, kcal mol^{-1}) values, which were estimated as

$\Delta G_{sol} = \Delta E_{sol(SMD)} + \Delta G_{(gas)correction}$, where $\Delta E_{sol(SMD)}$ refers to the calculated solvation single point energy and $\Delta G_{(gas)correction}$ refers to the calculated thermal correction in the gas phase for Gibbs free energies. 3D structures for the optimized stationary points were prepared using CYL view [33].

3. Results and Discussion

In light of the experimental mechanistic studies, three potential reaction pathways for Pd-catalyzed, Friedel-Crafts intermolecular acylation of arenes to ketones were tentatively proposed by Arndtsen B.A. and co-workers. As seen from Scheme 3, initially, the Pd-catalyzed, Friedel-Crafts intermolecular acylation reaction undergoes the oxidative addition of C–I bond of aryl iodides with $(CO)_nPd(0)$ to generate the intermediate **A**, $(CO)_nIPd(II)Ar$. Subsequent C–C bond formation may take place through the CO insertion into the Pd–C bond of Pd(II) intermediate **A** to give a palladium-aroyl intermediate **B**. Next, a substitution reaction between the aromatic silver and the palladium-aroyl intermediate **B** could occur to furnish intermediate **C**, followed by a reductive elimination to yield the product of ketone and regenerate the $(CO)_nPd(0)$ catalyst (Path I). Alternatively, silver trifluoromethanesulfonate reacts with intermediate **B** to give the monoxide coordinated Pd–COAr intermediate **D**. After formation of intermediate **D**, it may be sufficiently electrophilic to palladate benzene (Path II), or directly undergoes reductive elimination to give an aroyl triflate electrophile that reacts with arene to form the final product ketones and Pd(0) catalyst (Path III). Here, we report our DFT studies of all reaction mechanisms shown in the Scheme 3. We first investigated the formation of the palladium-aroyl intermediate **A**, $(CO)_nIPdAr$, via C–I bond oxidative addition with $(CO)_nPd(0)$ catalyst, followed by the CO insertion reaction to give intermediate **B**. Then, three alternative reaction pathways to afford the products of ketones were examined and compared. Finally, the aforementioned mechanistic issues were discussed in detail.

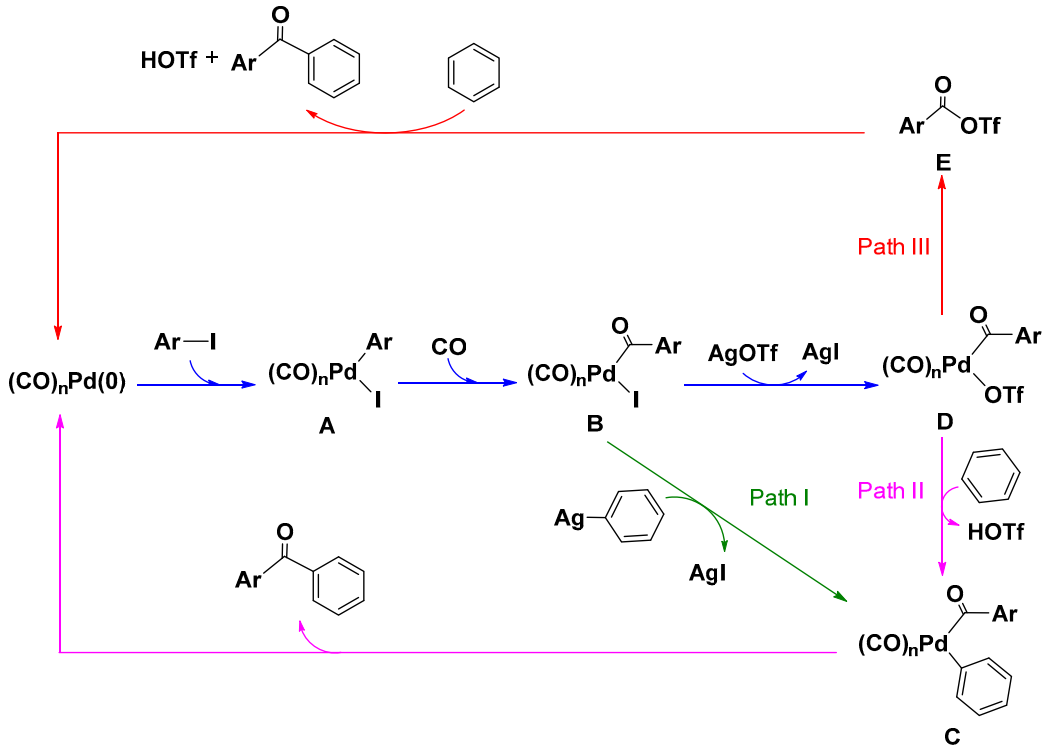

Scheme 3. Proposed reaction mechanism for Pd-catalyzed, Friedel-Crafts intermolecular acylation.

3.1. Mechanism

3.1.1. Mechanism of Forming Palladium-Aroyl Intermediate **B** from Reaction between $(CO)_nPd(0)$ and Aryl Iodide

For the formation of palladium-aroyl intermediate **B**, two possible reaction scenarios were examined when considering whether one CO is dissociative or associative over the course of reaction. The corresponding potential energy surfaces are depicted in Figure 1. The calculated results show that although extrusion of one CO molecule for the complexation of $(CO)_3Pd$ and aryl iodide is endergonic by 7.8 kcal mol^{-1}, its overall activation free energy required in the C–I bond oxidative addition reaction is lower than that in the case associated with one CO by 3.4 kcal mol^{-1} (23.2 vs. 26.6 kcal mol^{-1} for **TS1** vs. **TS1′**). Furthermore, the resultant intermediate **A** from the oxidative addition reaction with the dissociation of CO was also more stable than its counterpart by 10.9 kcal mol^{-1} (4.4 kcal mol^{-1} vs. 15.3 kcal mol^{-1} for **A** vs. **A′**). Subsequently, insertion of CO into the Pd–C bond of intermediate **A** and **A′** via **TS2** and **TS2′** requires overcoming reaction barrier of 6.5 and 15.9 kcal mol^{-1} with respect to the intermediate **A** to give palladium-aroyl intermediate **B** and **B′**, respectively. This indicates that intermediate **A** with two CO molecular ligands undergoes the insertion reaction is energetically favorable than intermediate **A′** with three CO molecules. However, we noted that the formation of palladium-aroyl intermediate **B′** is exergonic by 11.2 kcal mol^{-1}, which is much larger in energy than that (1.3 kcal mol^{-1}) of palladium-aroyl intermediate **B**. As such, one CO molecule was extruded before the C–I oxidative addition and then one CO molecule was incorporated after CO insertion into the Pd–C bond, which is important to provide the kinetic and thermodynamic driving forces during the course of reactions. The more energetically-favorable mechanism of dissociation than the associative one may lie in the fact that extrusion of an electron-deficient group of CO in the dissociative mechanism leads the coordinated palladium atom with more electrons, thus benefiting the oxidative addition process.

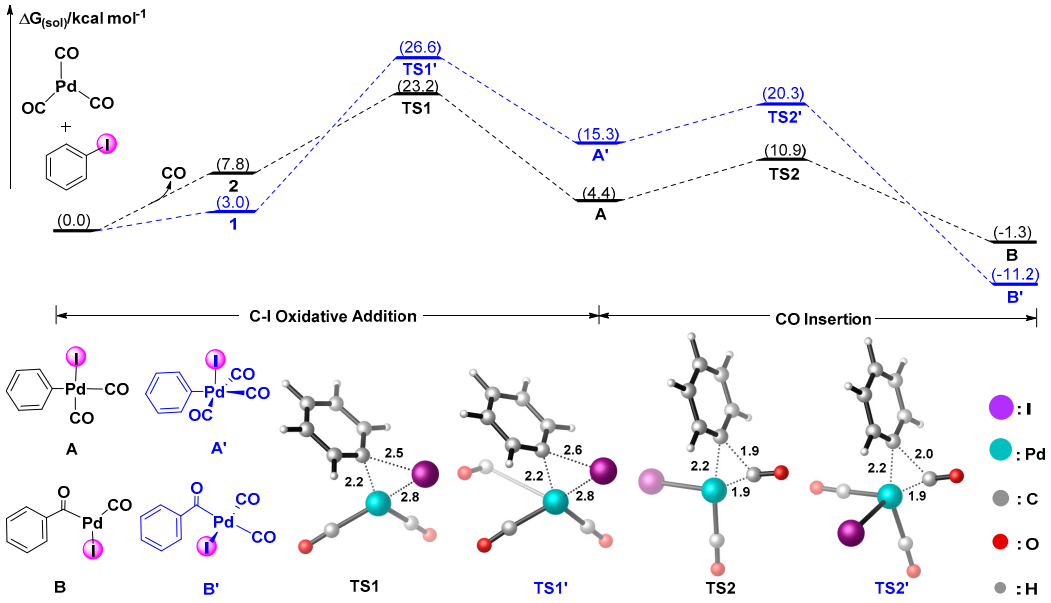

Figure 1. Computed reaction potential surfaces of formation of palladium-aroyl intermediate (associative mechanism in blue vs. dissociative mechanism in black).

3.1.2. Mechanism for the Formation of Ketones Derived from Aromatic Silver

When considering that aromatic silver was successfully synthesized and can also be involved in the C–H arylation of electron-deficient arenes as found in the experiments reported by some workers [34,35], the reaction of arylsilver with intermediate **B′** was initially calculated (Path I). As seen in Figure 2, the formation of ketones is very facile, both kinetically and thermodynamically, and

consists of exergonic ion exchange process (all attempts were failed to locate transition state) and reductive elimination with a small reaction barrier of 3.6 kcal mol^{-1}. However, this calculated finding leaves us an open-ended question: can the arylsilver be produced easily under the experimentally used reaction conditions? Here, we conducted a computational study of the reaction between aryl iodide and AgOTf with or without phosphine ligand. Both of them indicated that the generation of arylsilvers is prohibited by the extremely high reaction barriers of about 44 kcal mol^{-1} (Figures S1 and S2), and thus, arylsilver is less likely involved in the C–H bond activation of arenes. In order to verify our calculations, we further investigated the feasibility of forming analogous arylsilvers, such as those reported by Sanford and Larrosa groups [34,35], which showed that AgOPiv or $AgCO_2Ad$ with phosphine ligands plays an important role in the C–H cleavage step for the formation of related arylsilvers. Accordingly, our calculations revealed that AgOPiv or $AgCO_2Ad$ with phosphine ligands can easily react with substituted arenes, associated with accessible reaction barriers (See Figure S3 of Supporting Information). NBO analysis indicated that the C–H bond of arene substituted by electron-deficient moiety, such as F group, is more polarized (Table S1). As such, the presence of electron-deficient substituents on the arenes might account for the facile formation of these experimentally synthesized and characterized arylsilvers. Collectively, our calculated results demonstrated that although the ion exchange and reductive elimination processes take place efficiently for the formation of ketones (Figure 2), the generation of intermediate arylsilver requires very large reaction heights, and thus, the mechanism of forming an aroyl triflate electrophile derived from aromatic silver could be safely ruled out for the titled reaction.

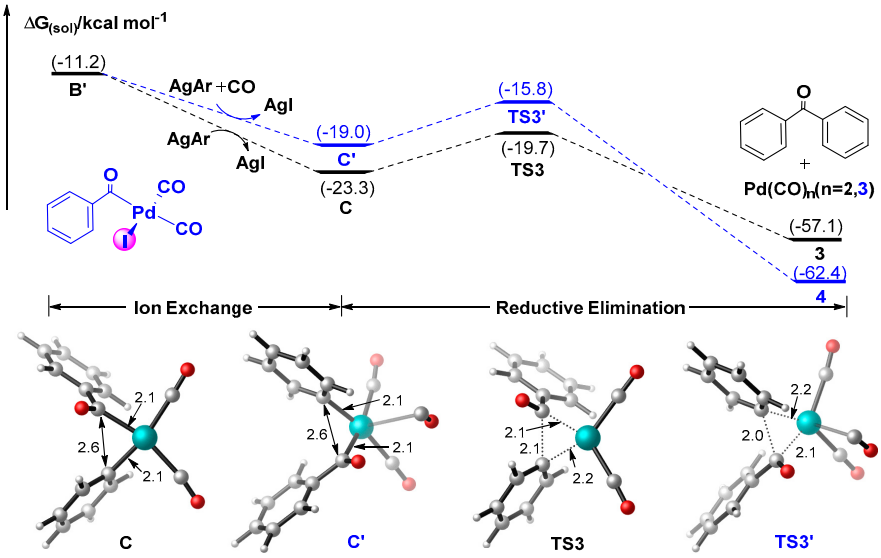

Figure 2. Reaction potential surfaces for the formation of ketones derived from aromatic silver.

3.1.3. Mechanism for the Formation of Ketones Involving Palladate Benzene

As shown in Figure 3, anion exchange between palladium-aroyl intermediate **B′** and AgOTf is an energetically downhill process to generate the palladium-aroyl intermediate **D** bearing triflate moiety, $[(CO)_2Pd(II)(COPh)OTf]$, and then it may undergo activation of the C–H bond of benzene as a sufficient electrophile to yield intermediate **E** (Path II) as suggested by Arndtsen B.A. et al. The calculated results show that such C–H activation proceeds via a four-membered transition state **TS4** or **TS4′**, and is characterized by a relatively high reaction barrier of 35.8 and 38.4 kcal mol^{-1}, respectively. Finally, the C–C bond formation to produce the ketones via reductive elimination is relatively facile and requires an activation free energy of 3.7 kcal mol^{-1}. Taken together, the calculations revealed that C–H bond activation of benzene by palladium-aroyl intermediate **D** bearing triflate moiety is the rate-limiting step for the formation of ketones, which is less likely to occur with respect to that via aroyl triflate (Path III, vide infra).

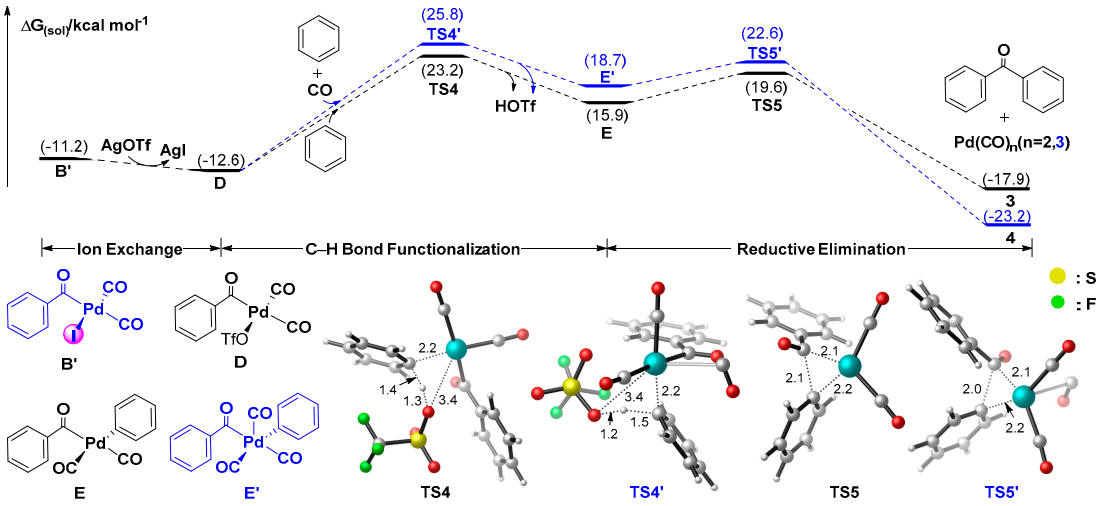

Figure 3. Calculated reaction potential surfaces for the formation of ketones catalyzed by palladium-aroyl intermediate.

3.1.4. Mechanism for the Formation of Ketones Delivered by Aroyl Triflate

From the palladium-aroyl intermediate **D**, $[(CO)_2Pd(II)(COPh)OTf]$, an alternative pathway is responsible for the formation of aroyl triflate and regeneration of the catalyst to enter the catalytic cycle. Additional calculations were conducted by considering the possible reductive elimination of the palladium-aroyl intermediate **D**, $[(CO)_2Pd(II)(COPh)OTf]$ and the C–H bond activation of arenes by the electrophilic attack of resultant aroyl triflate (depicted as path III in Figure 4). Calculations indicated that the reductive elimination of the palladium-aroyl intermediate **D** requires the reaction barrier of 18.4 kcal mol^{-1} via three-membered transition state **TS6** with C–O and O–Pd bond distance of 1.8 Å and 2.3 Å, respectively. It is noted that incorporation of one monoxide into $(CO)_2Pd(0)$ catalyst leads a more stable, three monoxide-coordinated $(CO)_3Pd(0)$ catalyst, thereby providing an additional driving force for such reductive elimination process. As a result, the generation of aroyl triflate and the $(CO)_3Pd(0)$ catalyst is exergonic by 7.9 kcal mol^{-1} with respect to species **D**. From species aroyl triflate, C–H bond functionalization of benzene to give the product of ketones and to release trifluoromethane sulfonic acid was conducted computationally. This electrophilic attack process requires an activation free energy of 32.1 kcal mol^{-1} via the four-membered transition state **TS7**, and is further exergonic by 6.3 kcal mol^{-1}. For clarity, the full potential free energy surface of all elementary reaction steps including C–I oxidative addition, CO insertion, reductive elimination and C–H bond functionalization were combined together and provided in Figure 5. When considering the whole channels, the C–H bond functionalization of benzene via the resultant aroyl triflate is the rate-limiting step in the Path III.

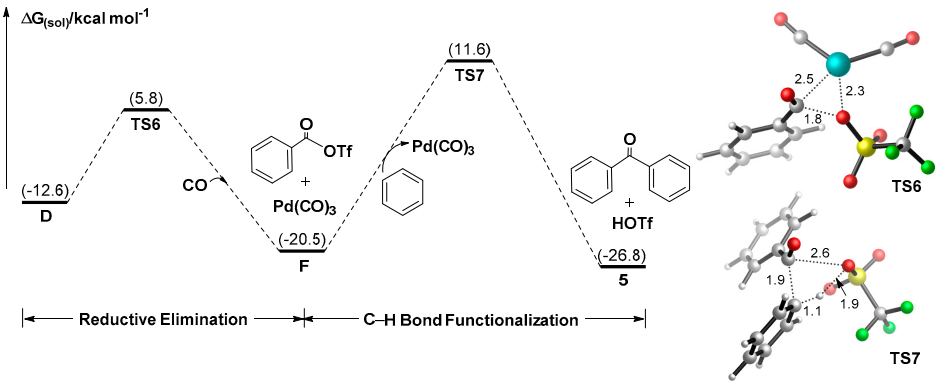

Figure 4. Reaction potential surfaces for the formation of ketones delivered by resultant aroyl triflate.

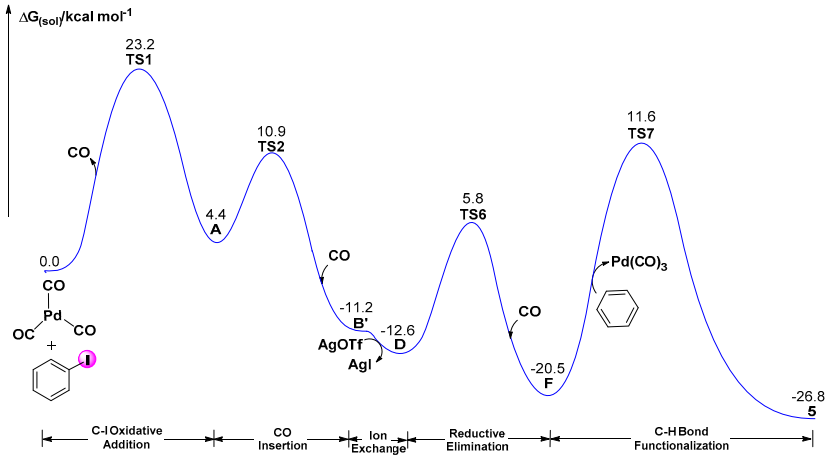

Figure 5. Full reaction potential energy surface of Path III.

As discussed above, Pd-catalyzed, Friedel-Crafts intermolecular acylation to ketones may take place via one of three potential pathways (Path I, II, and III). Our calculations indicated that after the formation of the palladium-aroyl intermediate **D** via C–I bond oxidative addition and CO insertion into Pd–C bond, the electrophilic reaction (C–H bond activation) of the resultant aroyl triflate with arene as the rate-determining step (Figure 5) is more energetically favorable than path II by 3.7 kcal mol^{-1} (Figure 4). However, our NBO analysis, which indicated that the O atom of OTf group in the palladium-aroyl intermediate **D** carries a larger negative charge than that of aroyl triflate species (-0.63 vs. -0.58), and thus, the former is more electrophilic to functionalize the C-H bond of benzene. This is in contrast to the calculated results shown in Figures 4 and 5. Therefore, we envisioned that the larger steric repulsion between the palladium-aroyl intermediate **D** and benzene should be considered in the electrophilic attacking reaction and might translate into the corresponding higher reaction height. Evidently, intermolecular carbonylation of the arene C–H bonds proceeds through the unprecedented palladium-catalyzed formation of aroyl triflates. This is consistent with the experimental findings that the experimental build up and isolation of aroyl triflates can react with benzene and give the desired ketone products. As such, the mechanism for the titled catalytic reaction via path III is most likely responsible for the formation of ketones.

3.2. Why are Pd Salts Superior to the Ligated Pd Complexes in Catalytic Activities?

It was experimentally shown that a non-ligated palladium catalyst is superior to the Pd catalyst bearing the phosphine ligands in term of the reactivity of intermolecular carbonylation of arene C–H bonds. For instance, carbonylative C–H functionalization of arenes to form ketones was not observed in the presence of Pd(^{t}Bu$_3$)$_2$, whereas simple palladium salt ($PdCl_2$) catalysts proceeded to the related carbonylative C–H functionalization reactions smoothly with high yields. Intrigued by this unusual ability, we have conducted computational studies to elucidate the origins of reactivity discrepancy of these two Pd catalysts. As seen from Figure 6, transformation of the resultant aroyl triflate to phosphine coordinated palladium-aroyl intermediate **G** is very facile, both kinetically and thermodynamically, and is associated with an accessible reaction barrier of 21.4 kcal mol^{-1} at ambient temperature and is exergonic by 4.3 kcal mol^{-1}. Thus, forming the aroyl triflate as a strong electrophilic intermediate to functionalize C–H bond of arenes from the palladium-aroyl intermediate with phosphine ligand is difficult (see the detailed computational results of reaction mechanism mediated by Pd(P^{t}Bu$_3$)$_2$ in Figure S4 [36]). This is mainly attributed to the fact that P^{t}Bu$_3$ group as an electron-donating group could inject more electrons into the palladium atom, and thus, the oxidative addition of electrophilic aroyl triflate prefers to take place on a Pd(0) catalyst with more electron-donating ligands to give to the palladium-aroyl intermediate. On the other hand, the calculation shows that the functionalization of C–H bond of arene mediated by aroyl

triflate or palladium-aroyl intermediate requires a very high reaction barrier of about 44 kcal mol^{-1} and is thermodynamically unfavorable. In contrast, reductive elimination to generate electrophilic aroyl triflate is facilitated by a Pd catalyst with electron-withdrawing group. Indeed, as seen from Figure 7, with assistant of HOTf and CO, palladium-aroyl intermediate **G** could easily be transformed to a CO-bound palladium-aroyl intermediate **H** by protonated phosphine and ligand exchange processes. This process affords CO-coordinated species **H**, which is more stable than phosphine coordinated palladium-aroyl intermediate **G** by 7.7 kcal mol^{-1}. The subsequent step corresponds to the reductive elimination of species **H** to produce strongly electrophilic aroyl triflate and regenerate three CO-coordinated palladium catalysts (Pd(CO)$_3$). Evidently, the reductive elimination process of a CO-bound palladium-aroyl intermediate **H** requires a small reaction barrier of 15.5 kcal mol^{-1}, and is further exergonic by 11.7 kcal mol^{-1}, as shown in Figure 7, indicating that Pd catalyst containing electron-deficient group (CO) preferentially proceeds the reductive elimination instead of oxidative addition process (see electronic densities of Pd atom for phosphine or CO-coordinated palladium-aroyl intermediates in Table S2 of Supporting Information). This is because CO, as an electron-deficient ligand, could reduce the electron density of palladium-aroyl intermediate **H**, being benefical to the reductive elimination of palladium-aroyl intermediate, rather than the corresponding reversible oxidative addition of aroyl triflate with Pd catalyst. It is generally assumed that the experimental generation of Pd(CO)$_3$ catalyst using simple Pd salts in the presence of CO is thermally facile; as such, the simple palladium salts with no added ligands would efficiently catalyze the intermolecular functionalization of benzene with CO, aryl iodide and a triflate source.

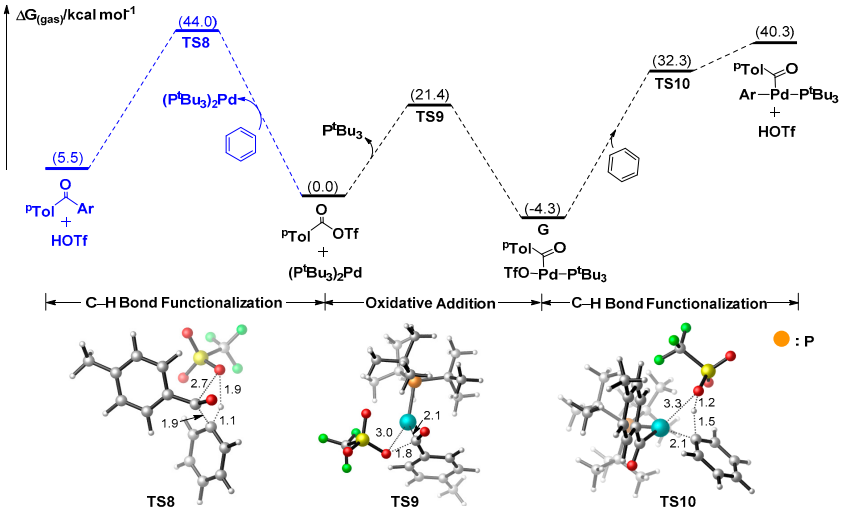

Figure 6. Calculated reaction potential energy surface of transformation between aroyl triflate or palladium-aroyl intermediate and the related C-H functionalization.

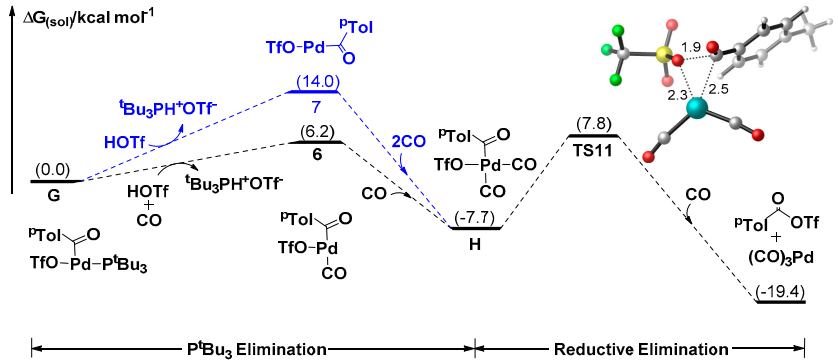

Figure 7. Calculated reaction potential energy surface of sequestrating P^{t}Bu$_3$ to generate aroyl triflate in presence of HOTf and monoxide.

4. Conclusions

In summary, three potential reaction pathways for Pd-catalyzed, Friedel-Crafts intermolecular acylation of arenes to ketones were systematically conducted by DFT calculations. The computational results indicated that an acylation reaction involving the aroyl triflate is the most preferred pathway where the arene C–H bond functionalization step was mediated by the strongly electrophilic aroyl triflate (Path III). It is noteworthy that not only the presence of CO is highly important as the carbonyl source, but also the dissociation and association of CO with Pd center provides the important kinetical and thermodynamic driving forces for the whole reaction. That is, the dissociation of CO molecule before oxidative addition increases the electron density and reduces the steric effect, which benefits C–I bond cleavage mediated by Pd catalyst. In contrast, the re-coordination of the CO molecule with the Pd atom after reductive elimination provides more thermodynamically driving force for the generation of electrophilic aroyl triflate. In addition, the calculation indicated that simple Pd salts possess unusual catalytic ability with respect to the ligated Pd catalyst ($Pd(P^tBu_3)_2$). This is in accordance with the experimental findings, likely owing to the presence of the electron-deficient group of CO that reduces the electron density of the Pd(II) complex and facilitates reductive elimination to provide the strong electrophilicity of aroyl triflate available for the subsequent C–H activation of arenes.

Supplementary Materials: The following are available online at http://www.mdpi.com/2073-4344/9/2/141/s1. 1. Computed reaction energy profile between aryl iodide and AgOTf with or without phosphine ligand in Arndtsen B.A. and co-workers' experiment, 2. Computed reaction energy profile of AgOPiv or AgCO2Ad with phosphine ligands reacting with substituted arenes reported by Sanford and Larrosa groups, 3. Computed reaction energy profile of on the main process catalyzed by the $Pd(PR_3)_3$, 4. NBO analysis of several structures, 5. Cartesian coordinates of all structures.

Author Contributions: R.C. performed the calculations; Y.T., N.L., J.B., H.Y. and W.Y. analyzed the data; Z.G. and Y.L. conceived the project and wrote the paper.

Acknowledgments: We acknowledge the financial support from the National Nature Science Foundation of China (No. 61775155); the 100–Talent Program in Shanxi Province, Taiyuan University of Science and Technology of China.

Conflicts of Interest: The authors declare no conflict of interest.

References

1. Hatano, B.; Kadokawa, J.I.; Tagaya, H. Disproportionation of diarylmethanol derivatives by using supercritical water. *Tetrahedron Lett.* **2002**, *43*, 5859–5861. [CrossRef]
2. Dieter, R.K. Reaction of acyl chlorides with organometallic reagents: A banquet table of metals for ketone synthesis. *Tetrahedron* **1999**, *55*, 4177–4236. [CrossRef]
3. Sharmoukh, W.; Ko, K.C.; Noh, C.; Lee, J.Y.; Son, S.U. Designed Synthesis of Multi–Electrochromic Systems Bearing Diaryl Ketone and Isophthalates. *J. Org. Chem.* **2010**, *75*, 6708–6711. [CrossRef] [PubMed]
4. Hartwig, J.F. Evolution of C–H Bond Functionalization from Methane to Methodology. *J. Am. Chem. Soc.* **2016**, *138*, 2–24. [CrossRef] [PubMed]
5. Lyons, T.W.; Sanford, M.S. Palladium–Catalyzed Ligand–Directed C–H Functionalization Reactions. *Chem. Rev.* **2010**, *110*, 1147–1169. [CrossRef] [PubMed]
6. Colby, D.A.; Bergman, R.G.; Ellman, J.A. Rhodium–Catalyzed C–C Bond Formation via Heteroatom–Directed C–H Bond Activation. *Chem. Rev.* **2010**, *110*, 624–655. [CrossRef] [PubMed]
7. Chen, X.; Engle, K.M.; Wang, D.H.; Yu, J.Q. Palladium(II)–Catalyzed C–H Activation/C–C Cross–Coupling Reactions: Versatility and Practicality. *Angew. Chem. Int. Ed.* **2009**, *48*, 5094–5115. [CrossRef] [PubMed]
8. Liu, C.; Yuan, J.W.; Gao, M.; Tang, S.; Li, W.; Shi, R.Y.; Lei, A.W. Oxidative Coupling between Two Hydrocarbons: An Update of Recent C–H Functionalizations. *Chem. Rev.* **2015**, *115*, 12138–12204. [CrossRef]
9. Cernak, T.; Dykstra, K.D.; Tyagarajan, S.; Vachal, P.; Krska, S.W. The medicinal chemist's toolbox for late stage functionalization of drug–like molecules. *Chem. Soc. Rev.* **2016**, *45*, 546–576. [CrossRef]
10. Olah, G.A. *Friedel-Crafts and Related Reactions*; Interscience Publishers-John Wiley & Sons, Inc.: London, UK; Beccles, UK, 1963; Volume 1.

11. Kuhl, N.; Hopkinson, M.N.; Wencel–Delord, J.; Glorius, F. Beyond Directing Groups: Transition–Metal–Catalyzed C–H Activation of Simple Arenes. *Angew. Chem. Int. Ed.* **2012**, *51*, 10236–10254. [CrossRef]
12. Hartwig, J.F.; Larsen, M.A. Undirected, Homogeneous C–H Bond Functionalization: Challenges and Opportunities. *ACS Cent. Sci.* **2016**, *2*, 281–292. [CrossRef] [PubMed]
13. Kinney, R.G.; Tjutrins, J.; Torres, G.M.; Liu, N.J.; Kulkarni, O.; Arndtsen, B.A. A general approach to intermolecular carbonylation of arene C–H bonds to ketones through catalytic aroyl triflate formation. *Nat. Chem.* **2018**, *10*, 193–199. [CrossRef] [PubMed]
14. Frisch, M.J.; Trucks, G.W.; Schlegel, H.B.; Scuseria, G.E.; Robb, M.A.; Cheeseman, J.R.; Scalmani, G.; Barone, V.; Mennucci, B.; Petersson, G.A.; et al. *Gaussian 09*; Revision E.01; Gaussian, Inc.: Wallingford, CT, USA, 2009.
15. Becke, A.D. Density–functional thermochemistry. I. The effect of the exchange–only gradient correction. *J. Chem. Phys.* **1992**, *96*, 2155–2160. [CrossRef]
16. Becke, A.D. Density–functional thermochemistry. II. The effect of the Perdew–Wang generalized–gradient correlation correction. *J. Chem. Phys.* **1992**, *97*, 9173–9177. [CrossRef]
17. Becke, A.D. Density–functional thermochemistry. III. The role of exact exchange. *J. Chem. Phys.* **1993**, *98*, 5648–5652. [CrossRef]
18. Lee, C.; Yang, W.; Parr, R.G. Development of the Colle–Salvetti correlation–energy formula into a functional of the electron density. *Phys. Rev. B Condens. Matter* **1988**, *37*, 785–789. [CrossRef] [PubMed]
19. Hariharan, P.C.; Pople, J.A. The influence of polarization functions on molecular orbital hydrogenation energies. *Theor. Chem. Acta* **1973**, *28*, 213–222. [CrossRef]
20. Dolg, M.; Wedig, U.; Stoll, H.; Preuss, H. Energy–adjusted ab initio pseudopotentials for the first row transition elements. *J. Chem. Phys.* **1987**, *86*, 866–872. [CrossRef]
21. Andrae, D.; Häußermann, U.; Dolg, M.; Stoll, H.; Preuß, H. Energy–adjusted ab initio pseudopotentials for the second and third row transition elements. *Theor. Chem. Acta* **1990**, *77*, 123–141. [CrossRef]
22. Fukui, K. The path of chemical reactions–the IRC approach. *Acc. Chem. Res.* **1981**, *14*, 363–368. [CrossRef]
23. Marenich, A.V.; Cramer, C.J.; Truhlar, D.G. Universal Solvation Model Based on Solute Electron Density and on a Continuum Model of the Solvent Defined by the Bulk Dielectric Constant and Atomic Surface Tensions. *J. Phys. Chem. B* **2009**, *113*, 6378–6396. [CrossRef] [PubMed]
24. Ramalho, J.P.P.; Gomes, J.R.B.; Illas, F. Accounting for van der Waals interactions between adsorbates and surfaces in density functional theory based calculations: Selected examples. *RSC Adv.* **2013**, *3*, 13085–13100. [CrossRef]
25. Zhao, Y.; Truhlar, D.G. A new local density functional for main–group thermochemistry, transition metal bonding, thermochemical kinetics, and noncovalent interactions. *J. Chem. Phys.* **2006**, *125*, 194101. [CrossRef] [PubMed]
26. Zhao, Y.; Truhlar, D.G. The M06 suite of density functionals for main group thermochemistry, thermochemical kinetics, noncovalent interactions, excited states, and transition elements: Two new functionals and systematic testing of four M06–class functionals and 12 other functionals. *Theor. Chem. Acc.* **2008**, *120*, 215–241.
27. Krishnan, R.; Binkley, J.S.; Seeger, R.; Pople, J.A. Self–consistent molecular orbital methods. XX. A basis set for correlated wave functions. *J. Chem. Phys.* **1980**, *72*, 650–654. [CrossRef]
28. Yang, Y.F.; Cheng, G.J.; Liu, P.; Leow, D.; Sun, T.Y.; Chen, P.; Zhang, X.; Yu, J.Q.; Wu, Y.D.; Houk, K.N. Palladium–Catalyzed Meta–Selective C–H Bond Activation with a Nitrile–Containing Template: Computational Study on Mechanism and Origins of Selectivity. *J. Am. Chem. Soc.* **2014**, *136*, 344–355. [CrossRef] [PubMed]
29. Yang, Y.M.; Dang, Z.M.; Yu, H.Z. Density functional theory investigation on Pd–catalyzed cross–coupling of azoles with aryl thioethers. *Org. Biomol. Chem.* **2016**, *14*, 4499–4506. [CrossRef]
30. Anand, M.; Sunoj, R.B.; Schaefer, H.F. Palladium–Silver Cooperativity in an Aryl Amination Reaction through C–H Functionalization. *ACS Catal.* **2016**, *6*, 696–708. [CrossRef]
31. Zhou, M.J.; Yang, T.L.; Dang, L. Theoretical Studies on Palladium–Mediated Enantioselective C–H Iodination. *J. Org. Chem.* **2016**, *81*, 1006–1020. [CrossRef]
32. Liu, L.; Liu, Y.; Ling, B.; Bi, S. Mechanistic investigation into Et_3N C–H activation and chemoselectivity by Pd–Catalyzed intramolecular heck reaction of N–Vinylacetamides. *J. Organomet. Chem.* **2017**, *827*, 56–66. [CrossRef]

33. Legault, C.Y. *CYLView, 1.0b*; Université de Sherbrooke: Sherbrooke, QC, Canada, 2009; Available online: http://www.cylview.org (accessed on 2 December 2018).
34. Lotz, M.D.; Camasso, N.M.; Canty, A.J.; Sanford, M.S. Role of Silver Salts in Palladium–Catalyzed Arene and Heteroarene C–H Functionalization Reactions. *Organometallics* **2017**, *36*, 165–171. [CrossRef]
35. Whitaker, D.; Burés, J.; Larrosa, I. Ag(I)–Catalyzed C–H Activation: The Role of the Ag(I) Salt in Pd/Ag–Mediated C–H Arylation of Electron–Deficient Arenes. *J. Am. Chem. Soc.* **2016**, *138*, 8384–8387. [CrossRef] [PubMed]
36. Joost, M.; Zeineddine, A.; Estevez, L.; Ladeira, S.M.; Miqueu, K.; Amgoune, A.; Bourissou, D. Facile Oxidative Addition of Aryl Iodides to Gold(I) by Ligand Design: Bending Turns on Reactivity. *J. Am. Chem. Soc.* **2014**, *136*, 14654–14657. [CrossRef] [PubMed]